

Rotational mixing in early-type stars: the main-sequence evolution of a $9 M_{\odot}$ star.

Suzanne Talon¹, Jean-Paul Zahn¹, André Maeder² and Georges Meynet²

¹ Département d’Astrophysique Stellaire et Galactique, Observatoire de Paris, Section de Meudon, 92195 Meudon, France

² Observatoire de Genève, CH-1290, Sauverny, Switzerland

e-mail : talon@obspm.fr, zahn@obspm.fr, maeder@scsun.unige.ch, meynet@scsun.unige.ch

March 27, 2018

Abstract. We describe the main-sequence evolution of a rotating $9 M_{\odot}$ star. Its interior rotation profile is determined by the redistribution of angular momentum through the meridian circulation and through the shear turbulence generated by the differential rotation; the possible effect of internal waves is neglected. We examine the mixing of chemicals produced by the same internal motions. Our modelization is based on the set of equations established by Zahn (1992) and completed in Matias, Talon & Zahn (1996). Our calculations show that the amount of mixing associated with a typical rotation velocity of $\sim 100 \text{ km s}^{-1}$ yields stellar models whose global parameters are very similar to those obtained with the moderate overshooting ($d/H_P \simeq 0.2$) which has been invoked until now to fit the observations. Fast rotation ($\sim 300 \text{ km s}^{-1}$) leads to significant changes of the C/N and O/N surface ratios, but the abundance of He is barely increased. The modifications of the internal composition profile due to such rotational mixing will certainly affect the post-main-sequence evolution.

Key words: Stars: abundances, early-type, evolution, interior, rotation.

Indeed it is well known, since the early work of Eddington (1925) and Vogt (1925), that the meridional currents arising in a rotating star may cause internal mixing. But until recently, the only case considered seriously was that of uniformly rotating stars, and it has been proved by Messtel (1953) that in such stars the stabilizing effect of the composition gradients, which arise from hydrogen burning, is so strong that even the fastest rotators are unlikely to be mixed.

The situation is different, however, if one allows the circulation to modify the rotation profile, as has been pointed out by Zahn (1992; Paper I). He invoked the anisotropic turbulence observed in stratified fluids, with much stronger transport in the horizontal than in the vertical direction, to reduce the problem to one dimension, with the angular velocity Ω depending only on depth. Then the evolution of Ω obeys a “hyper-diffusion” equation, involving the fourth derivative of Ω , and in massive main-sequence stars the rotation profile tends to adjust such as to minimize the flux of angular momentum, as had been anticipated by Busse (1981). Provided there is no interference from other transport processes, the residual turbulence associated with that differential rotation is the main cause of mixing in the radiative interior, and this is true even in the regions of strong composition gradient which arise near the convective core, thanks to the homogenizing action of the anisotropic turbulence, as shown recently by Talon & Zahn (1996).

Other groups have worked on rotational mixing in early-type stars, and they have clearly shown that such mixing may modify the surface abundances of He, C, N and O (Langer 1991, 1992; Denissenkov 1994; Eryurt et al. 1994). However, they have used an older prescription based largely on dimensional arguments, which links that mixing to the rotation velocity (Zahn 1983). Meynet & Maeder (1996) performed similar calculations, but they took into account differential rotation, and calculated the diffusion related to it, assuming that the rotation profile is determined by the local conservation of angular mo-

1. Introduction

There are many reasons to suspect that the amount of mixing presently included in stellar models, in the form of overshooting or semi-convection, is insufficient to explain some observational facts (Maeder 1995). In particular, Herrero et al. (1992) found a strong correlation between He enrichment and surface velocity in O-type stars, which indicates that there is probably a link between rotation and mixing.

Send offprint requests to: S. Talon

mentum. The improvement brought by the present paper is that here the internal rotation evolves for the first time consistently under the combined action of the meridional circulation and the shear turbulence. Furthermore, as explained in Zahn (1992) and in Matias et al. (1996), our treatment of rotational mixing involves only one free parameter, which we hope to calibrate in the near future using fast rotators.

In this paper our goal is more modest, for we shall not consider stars as massive as those observed by Herrero et al. The main reason is that we do not want our results to depend too drastically on the prescription employed to treat semi-convection, which significantly affects the structure of the inner portion of O-stars. We choose to describe the evolution of a $9 M_{\odot}$ star, and intend to compare our results with the observations used to calibrate overshooting in moderate mass stars.

We begin by presenting our stellar models and the equations governing the transport of angular momentum and of chemical elements (§2). The results for a hypothetical, stationary model are discussed in (§3), and those for the full main-sequence evolution in (§4).

2. Stellar models with rotation

2.1. Input physics

Our models were built with the Geneva stellar evolution code, and they were evolved starting from a homogeneous composition at the zero-age main-sequence (ZAMS).

The equation of state includes partial ionization close to the surface of the star.

We used the OPAL radiative opacities (Iglesias et al. 1992) which include the spin-orbit interactions for Fe. The relative metal abundances are based on Grevesse (1991), consistently with the opacity used. Note however that this consistency will be lost in the course of evolution, since mixing and nuclear processing modify those relative abundances. The tables are completed for the lower temperatures (below 10 000K) by those given by Kurucz (1991).

Hydrogen burning proceeds through the p-p chains and the CNO cycle. The reaction rates are as given by Caughlan & Fowler (1988) with the correction by Landré et al. (1990) for the reactions $^{17}\text{O}(p, \gamma)^{18}\text{F}$ and $^{17}\text{O}(p, \alpha)^{14}\text{N}$.

For the mixing length parameter $\alpha = l/H_P$ we take the value 1.6, drawn from the solar calibration with the same code (cf. Schaller et al. 1992).

No allowance will be made here for convective penetration, which is still a matter of debate. Most theoretical predictions (Roxburgh 1978, 1989; Zahn 1991) tend to overestimate this penetration, and the reason may be that they do not account for the inhibiting effect of rotation, which has been clearly demonstrated in the recent numerical simulations performed by Julien et al. (1996).

One important observational constraint for models of OB stars is the width of the main-sequence, and it can be

accounted for by an overshooting parameter $d/H_p \simeq 0.2$ (cf. Stothers & Chin 1991). However, this value characterizes in fact the size of the well mixed core of the star, and that mixing may be due either to convective penetration or to any other mechanism. In this study, we shall examine whether this core extension may be attributed to rotational mixing, as described by Zahn's formalism (cf. Paper I). Therefore, we assume that convective overshooting is rather weak, just enough to yield a finite value of the subadiabatic gradient ($\nabla_{\text{ad}} - \nabla_{\text{rad}}$), in order to prevent the divergence of the circulation velocity at the boundary of the convective core.

Mass loss is also included, following the empirical relation given by de Jager et al. (1988), which is valid for O to M main-sequence stars.

Furthermore, the equilibrium structure of our models includes the mean centrifugal force (averaged over an isobar). The hydrostatic equation reads:

$$\frac{1}{\rho} \frac{dP}{dr} = -\frac{Gm}{r^2} + \frac{1}{2} \langle \sin^2 \theta \rangle \Omega^2 r \quad (1)$$

where we use standard notations for the pressure (P), density (ρ), radius (r), mass (m), gravitational constant (G), colatitude (θ), angular velocity (Ω) and where the horizontal average of f is defined as

$$\langle f \rangle = \frac{\int_0^\pi f \sin \theta d\theta}{\int_0^\pi \sin \theta d\theta}. \quad (2)$$

We shall not refine here the implementation of the centrifugal force, since it would have little effect on mixing; for a more rigorous treatment, we refer the reader to Meynet & Maeder (1996), where they adapt the Kippenhahn & Thomas (1970) method to incorporate the hydrostatic effects of rotation in one dimension to the case of shellular rotation.

2.2. Transport equations

In this paper, we shall consider only the transport of matter and angular momentum due to meridional circulation and shear turbulence. Microscopic diffusion has negligible effect in early-type stars, and it will be ignored here. The possible redistribution of angular momentum through internal waves is also neglected, although it has been shown to play an important role in the Sun (Kumar & Quataert 1996; Zahn, Talon & Matias 1996); we shall revisit the problem once we dispose of a reliable prescription for this transport in a rapidly rotating star.

The equations controlling the evolution of the rotation profile through meridional advection and turbulent diffusion have been presented in Paper I and in Matias et al. (1996). Let us recall that the main assumption in this description is the strong anisotropy of the turbulence, whose horizontal transport enforces a state of shellular rotation

$\Omega = \Omega(P)$, so that all variables may be expressed with respect to the isobars as

$$\begin{aligned} f(P, \theta) &= \langle f(P, \theta) \rangle + \tilde{f}(P)P_2(\cos \theta) \\ &= f(P) + \tilde{f}(P)P_2(\cos \theta). \end{aligned} \quad (3)$$

After performing the suitable horizontal means, the transport equation for angular momentum is cast into

$$\rho \frac{\partial}{\partial t} [r^2 \Omega] = \frac{1}{5r^2} \frac{\partial}{\partial r} [\rho r^4 \Omega U] + \frac{1}{r^2} \frac{\partial}{\partial r} \left[\rho \nu_v r^4 \frac{\partial \Omega}{\partial r} \right] \quad (4)$$

(cf. Eq. (2.7) of Paper I), where ν_v is the vertical (turbulent) viscosity and U the amplitude of the vertical circulation speed $u(P, \theta) = U(P)P_2(\cos \theta)$:

$$U(P) = \frac{L}{mg} \left(\frac{P}{C_P \rho T} \right) \frac{1}{\nabla_{\text{ad}} - \nabla} [E_\Omega + E_\mu], \quad (5)$$

with L being the luminosity, g the local gravity, C_P the specific heat, T the temperature. The function E_Ω depends on the velocity profile

$$\begin{aligned} E_\Omega &= 2 \left[1 - \frac{\Omega^2}{2\pi G \rho} - \frac{\varepsilon}{\varepsilon_m} \right] \frac{\tilde{g}}{g} \\ &\quad - \frac{\rho_m}{\rho} \left[\frac{r}{3} \frac{\partial}{\partial r} \left(H_T \frac{\partial \Theta}{\partial r} - \chi_T \Theta \right) - 2 \frac{H_T}{r} \Theta + \frac{2}{3} \Theta \right] \\ &\quad - \frac{\varepsilon}{\varepsilon_m} \left[H_T \frac{\partial \Theta}{\partial r} + (\varepsilon_T - \chi_T) \Theta \right] \end{aligned} \quad (6)$$

and E_μ , on the chemical inhomogeneities along isobars

$$\begin{aligned} E_\mu &= \frac{\rho_m}{\rho} \left[\frac{r}{3} \frac{\partial}{\partial r} \left(H_T \frac{\partial \Lambda}{\partial r} - (\chi_T + 1) \Lambda - \sum_i \chi_{c_i} \frac{\tilde{c}_i}{c_i} \right) \right. \\ &\quad \left. - 2 \frac{H_T}{r} \Lambda \right] + \frac{\varepsilon}{\varepsilon_m} \left[H_T \frac{\partial \Lambda}{\partial r} + (\varepsilon_T - \chi_T - 1) \Lambda \right. \\ &\quad \left. + \sum_i (\varepsilon_{c_i} - \chi_{c_i}) \frac{\tilde{c}_i}{c_i} \right] \end{aligned} \quad (7)$$

(cf. Matias et al. 1996). Here ε is the nuclear energy generation rate, H_T the temperature scale height, χ the radiative conductivity, and c_i the concentration of a chemical species of mass number i ; the subscript m designates the mean value of the considered variable over the isobar, and other subscripts refer to logarithmic derivatives. $\Theta = r^2/3g\partial\Omega^2/\partial r$ is a measure of the differential rotation in the vertical direction and $\Lambda = \tilde{\mu}/\mu$ is the variation amplitude of the mean molecular weight along an isobar. This amplitude is derived from the horizontal variation of the concentration \tilde{c}_i of each species, which results from the competition between horizontal diffusion and vertical advection:

$$\tilde{c}_i = -\frac{r^2 U}{6 D_h} \frac{\partial c_i}{\partial r}. \quad (8)$$

The consequence is that the vertical transport due to the meridional circulation is turned into a diffusion, with an effective diffusivity given by (Chaboyer & Zahn 1992):

$$D_{\text{eff}} = \frac{|rU(r)|^2}{30 D_h}. \quad (9)$$

Thus the transport of a given chemical element varies with time according to

$$\rho \frac{\partial c_i}{\partial t} = \dot{c}_i + \frac{1}{r^2} \frac{\partial}{\partial r} \left[r^2 \rho (D_{\text{eff}} + D_v) \frac{\partial c_i}{\partial r} \right], \quad (10)$$

where the nuclear production/destruction rate \dot{c}_i is taken from the stellar structure code.

In this study, the only contribution retained in the *vertical* turbulent diffusivity (D_v) is that of the vertical shear, and we assume that this diffusivity equals the turbulent viscosity. We use the prescription given by Talon & Zahn (1996):

$$\nu_v = D_v = \frac{8 Ri_c}{5} \frac{(r \, d\Omega/dr)^2}{N_T^2/(K + D_h) + N_\mu^2/D_h}, \quad (11)$$

which takes into account the homogenizing effect of the horizontal diffusion (D_h) on the restoring force produced by the μ -gradient. Here, the Brunt-Väisälä frequency has been split into $N_T^2 = \frac{g\delta}{H_P} (\nabla_{\text{ad}} - \nabla)$ and $N_\mu^2 = \frac{g\varphi}{H_P} \nabla_\mu$, K is the radiative diffusivity and $Ri_c \approx 1/4$ is the critical Richardson number.

It remains to evaluate the magnitude of the horizontal diffusion (D_h), which we are unable to derive from first principles. We will use a parametric relation established as follows. Since the horizontal shear is sustained by the advection of momentum, D_h must be related to the circulation velocity U in order to keep the differential rotation in latitude below a certain level. This leads to

$$D_h = \frac{rU}{C_h} \left[\frac{1}{3} \frac{d \ln \rho r^2 U}{d \ln r} - \frac{1}{2} \frac{d \ln r^2 \Omega}{d \ln r} \right], \quad (12)$$

where C_h is an unknown parameter of order unity (see Zahn 1992).

2.3. Numerical technique

At each time step, the stellar evolution code is used to compute the mean structure of the model. Then, the meridional circulation is calculated, with the induced diffusion. The new rotation profile, as well as the new chemical abundances, are then implemented back into the evolutionary code, and we iterate until we reach the solution.

The fourth order equation governing the evolution of the rotation profile is solved by a relaxation method based on finite differences, as in the Henyey method employed in the stellar evolution code (cf. Henyey et al. 1964).

The diffusion equation is solved from the center of the star up to the surface, with a finite element method, using a semi-implicit temporal integration. The convective zone is homogenized by diffusion, using an arbitrary (large) coefficient of $D = 10^{14} \text{cm s}^{-1}$.

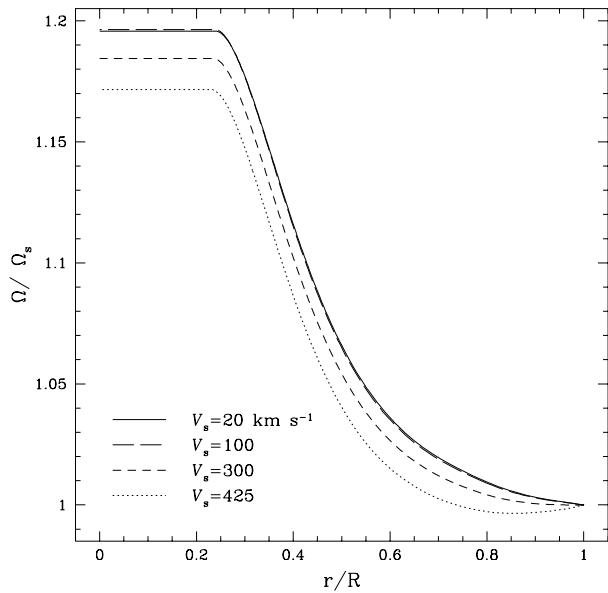


Fig. 1. Normalized rotation profiles in the asymptotic regime, for a $9M_{\odot}$ star. The solid line represents the star with a surface velocity of 20 km s^{-1} , the long dashed line the same with a velocity of 100 km s^{-1} , the short dashed line with a velocity of 300 km s^{-1} and the dotted line, the fastest rotator with a surface velocity of 425 km s^{-1} .

3. Asymptotic regime

When the star does not lose angular momentum, which to first approximation is the case of massive stars, the internal rotation rate tends to a profile which cancels the flux of angular momentum in the radiative interior. If the star was not evolving, the flow would settle into a stationary regime, in which the advection of angular momentum by the circulation exactly balances the diffusive transport:

$$-\frac{1}{5}U(P) = \nu_v \frac{d \ln \Omega}{dr}. \quad (13)$$

Although this state will never be achieved in a real star, it is worth considering it for the purpose of comparison with other results.

3.1. Asymptotic circulation profile in realistic models

We calculated the stationary regime obtained for a ZAMS star of $9M_{\odot}$. For this, we solved the p.d.e. (fourth order in space, first order in time) governing the evolution of angular momentum (Eq. 4), starting from solid body rotation, until we reached a stationary regime. Urpin et al. (1996) performed a similar study, for $20M_{\odot}$ models. However, they used a procedure slightly different from ours, searching directly the solutions of the third order o.d.e. (13). We shall compare our results to theirs when possible.

In Fig. 1, we show the rotation profiles obtained for four different surface velocities (20 , 100 , 300 and

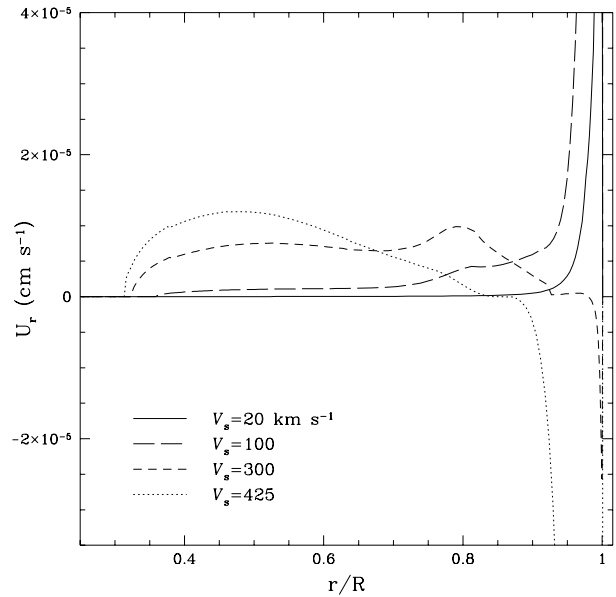


Fig. 2. Circulation velocity in the radial direction $U(r)$, for the asymptotic regime. (Line styles are defined as in Fig. 1.)

425 km s^{-1}). Figure 2 displays the corresponding radial velocities of the meridian circulation.

We observe that the normalized profile is independent of the rotation velocity in the inner portion of the star, whereas the situation is quite different close to the surface. The reason is that ν_v scales as Ω^2 , and so does also E_{Ω} , through \tilde{g}/g and Θ , as long as the next order term $-\Omega^2/2\pi G\rho$ remains negligible compared to unity, which is the case in the deep interior (cf. Eq. 6). Then Eq. (13) is insensitive to the magnitude of Ω , and it can only determine the shape of the rotation profile. That higher order term, which we owe to Gratton (1945) and Öpik (1951), dominates however near the surface, and it renders E_{Ω} nonlinear in Ω^2 , thus modifying the rotation profile. For rapid rotation, the radial derivative of Ω becomes positive near the surface, imposing a reversal of the diffusive flux and therefore also of the radial component of the circulation velocity, as can be seen in Fig. 2.

Urpin et al. reach similar conclusions. They obtain a differential rotation between center and surface of $\simeq 1.15$, which is comparable to what we get. Their fastest rotator (#4) corresponds to our model with 300 km s^{-1} . Its circulation velocity becomes marginally negative near the surface, as for ours. However, the velocities they obtain for the inner part of their models ($\sim 50 \text{ cm s}^{-1}$) imply viscosities of order $\sim 10^{12} \text{ cm}^2 \text{ s}^{-1}$, values that we do not reach.

Figure 3 displays the diffusion coefficients $D = D_{\text{eff}} + D_v + D_{\text{rad}}$ in the asymptotic regime (D_{rad} is the radiative viscosity). In the 300 and the 425 km s^{-1} models, we notice a sharp drop in D around $r/R \simeq 0.95$ and 0.85

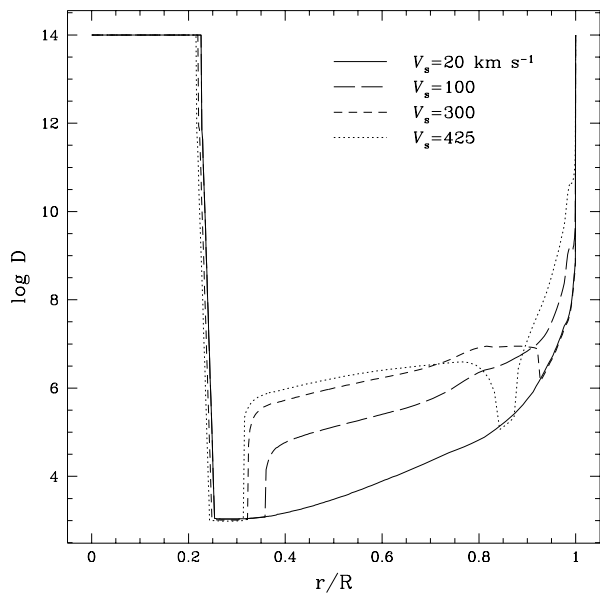


Fig. 3. Diffusion coefficients in the asymptotic regime. (Line styles are defined as in Fig. 1.)

respectively. It corresponds to the place where the derivative of Ω vanishes and thus, where no turbulence occurs. There, the viscosity is purely radiative and the transport of heavy elements will be strongly hindered. One could be tempted to conclude that, for the fastest stars, there will be two partially mixed zones, separated by a gap where very little diffusion takes place. Even worse, the region just outside of the convective core is not turbulent either, the diffusion coefficients diminishing by one or two orders of magnitude there. But we shall see in the next section that these conclusions are strongly affected by the structural changes accompanying the evolution, in particular by the chemical composition gradients.

Figure 3 illustrates yet another property of such rotating models, namely that the size of their convective core depends on rotation, with the fastest model having the smallest core. This is in agreement with previous studies of rotating stars (cf. e.g. Clement 1979), which predicted a lower central temperature and a smaller convective core for a rotating star than for a non-rotating one.

4. Circulation and evolution

The problem described in the previous section is rather academic. It is merely a guide to understand some basic properties of the circulation. However, it gives no clue as to what will happen actually to an evolving model, and it bypasses the important role of the μ -gradients.

As is well known, the radius of early-type stars increases as they evolve on the main-sequence. However, this expansion does not proceed in an homologous way,

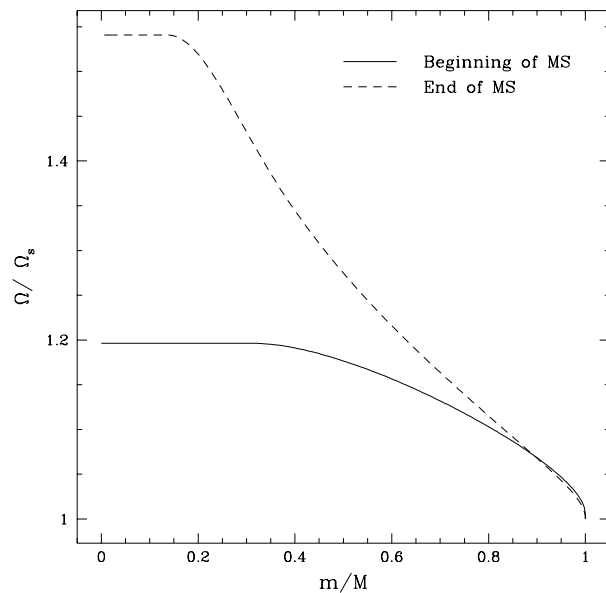


Fig. 4. Rotation profile required by thermal equilibrium; comparison between a ZAMS model and a TAMS model.

for the inner part is shrinking instead. Local conservation of angular momentum would lead to a core rotating much faster than the surface. Since the profile of Ω required by the asymptotic regime does not change much between consecutive models, we thus expect a circulation to arise that transports momentum from the center of the star to the surface. Such a circulation will rise along the equator and descend along the pole. Note that in a rigidly rotating star the circulation would be in the opposite direction (Sweet 1950).

In Fig. 4 we show the rotation profile required for this hypothetical stationary regime at the end of the main-sequence, compared to that on the ZAMS, for a model with an initial surface velocity of 100 km s^{-1} . It illustrates the need to carry angular momentum outward, since local conservation of angular momentum would lead to a differential rotation ratio (Ω_c/Ω_s) of order ~ 10 . (Note that on the TAMS, the total radius of the star has doubled compared to the ZAMS model).

Mass loss is also an important cause of circulation. The constant readjustment of the surface layers, which have to keep moving outward as the star loses mass, involves an important circulation in the outer part of the envelope. We thus expect outer layers to remain well mixed.

As was mentioned before though, the main impact of evolution is felt through the formation of a mean molecular weight gradient. In an inhomogeneous star, the relevant quantity in the description of the circulation is not Ω itself, but rather $\Theta - \Lambda$ (cf. Eq. 5). As was first shown by Mestel (1953), the advection of matter of larger mean molecular weight from the center of the star has a chok-

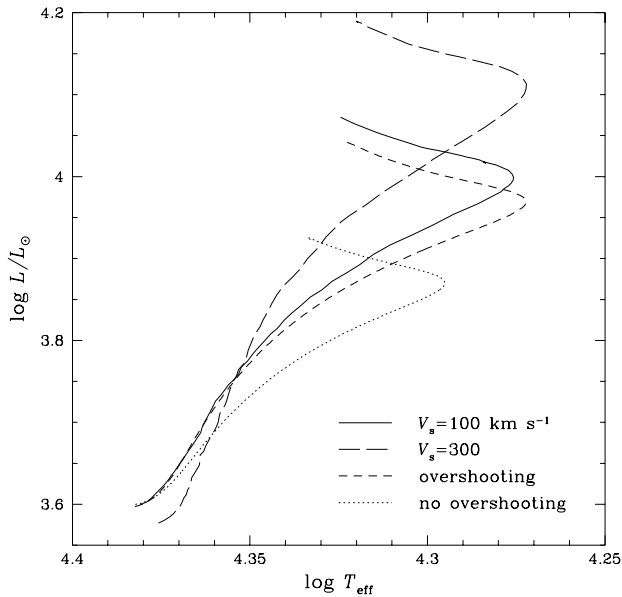


Fig. 5. The evolution of a rotating star of $9 M_{\odot}$ in the HR diagram. The solid line tracks the evolution of a star with an initial surface velocity of 100 km s^{-1} , the long dashed line that of a star with an initial surface velocity of 300 km s^{-1} . For reference, the short dashes show the evolution of the same star with an overshooting of $d/H_p = 0.2$ and the dotted line the star without any overshooting.

ing effect on the circulation. This, of course, is particularly important near the regressing convective core. However, contrary to Mestel’s conclusions, the circulation is not completely “killed” by those gradients, even though we expect it to be slowed. In an evolving star, the horizontal μ -gradients keep adjusting themselves to the new equilibrium state; furthermore, due to the erosion by the horizontal turbulence, at least a little amount of advection is required to maintain the horizontal inhomogeneities.

Another critical effect of the μ -gradients is that they tend to inhibit baroclinic shear instabilities. However, as was shown by Talon & Zahn (1996), if the turbulence is strongly anisotropic, horizontal diffusion reduces the buoyancy force associated with these gradients, just like temperature gradients are weakened by thermal diffusion. Their prescription (11) allows for vertical mixing, provided the differential rotation is strong enough.

4.1. Evolutionary calculations

Complete evolutionary calculations were performed for two models, initially rotating at 100 and 300 km s^{-1} (we will later refer to these models as “slow” and “fast”). The stars are assumed to be in the asymptotic regime on the ZAMS, thus having the rotation profiles shown in Fig. 1. We are aware that this initial condition is arbitrary,

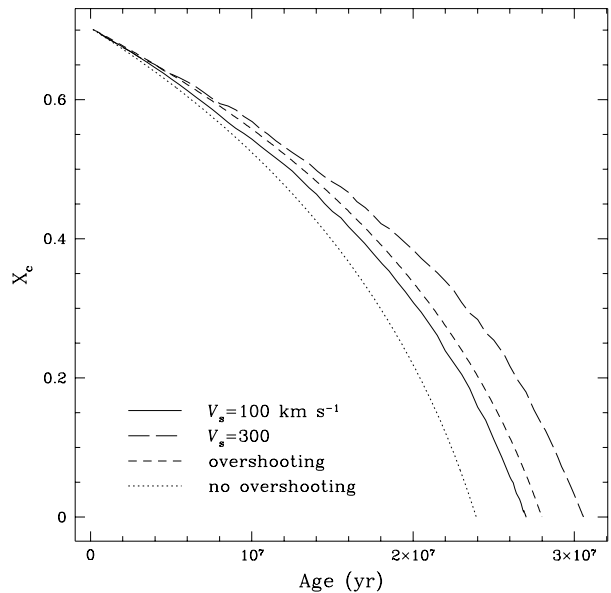


Fig. 6. Evolution of the central abundance of hydrogen. (Line styles are defined as in Fig. 5.)

but the memory of the initial condition will be lost in an Eddington-Sweet time-scale

$$t_{\text{ES}} = \frac{GM^2}{LR} \left(\frac{GM}{\Omega^2 R^3} \right), \quad (14)$$

of order 10^6 years for the considered models. Furthermore, during this early adjustment phase, no chemical inhomogeneities are present, and this diminishes the impact of the initial condition on the amount of mixing.

In Fig. 5, we show the evolutionary paths followed by the two models, plus that of two comparison models, one with a convective overshooting of $d/H_p = 0.2$, and the other one without overshooting. One striking feature of that diagram is that the mixing associated with a star initially rotating at 100 km s^{-1} yields an evolutionary path which can hardly be distinguished from that of a model with a small amount of overshooting. The initial positions of these models on the HR diagram also illustrate the small impact of the hydrostatic corrections on the global parameters, compared to those related to mixing.

At the end of the main-sequence, the “slow” model has lost 0.09% of its initial mass, and 1.4% of its total angular momentum. The “fast” model has lost 0.12% and 2.3% of its mass and momentum respectively. Remember that we used an empirical formula for mass loss that does not take into account the rotation rate of the star. The difference in the mass lost only reflects different lifetimes and effective temperatures during the evolution.

Figure 6 displays the evolution of the central mass fraction of hydrogen, and thus also the lifetime on the main-sequence. For the “slow” model, which has a velocity typ-

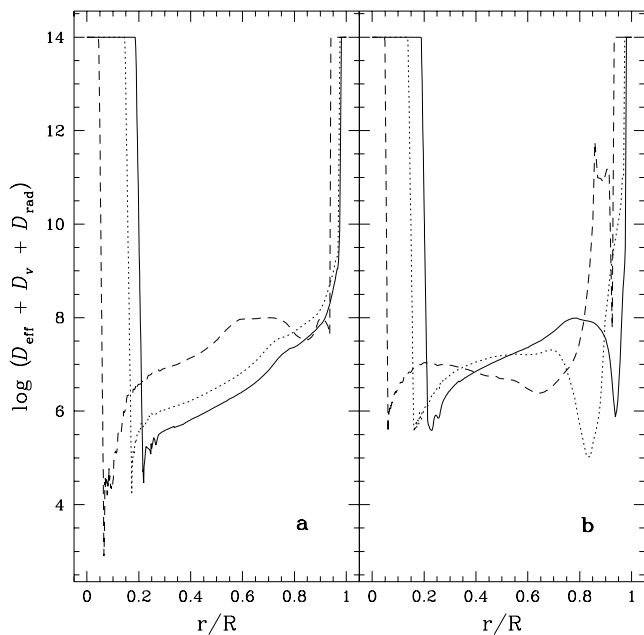


Fig. 7. Total diffusion coefficient and its variation with evolution. (a) Model with an initial surface velocity of 100 km s^{-1} . (b) Model with an initial surface velocity of 300 km s^{-1} . The full line refers to the youngest model, the dotted line to the model in the middle of the main-sequence, and the dashed line to the oldest model, at the turning point of the main-sequence.

ical for observed $9 M_{\odot}$ stars, the evolution in the HR diagram, as well as the main-sequence lifetime, are comparable to what is obtained with a standard model including overshooting.

As mentioned in the Introduction, convective penetration may be severely hindered in rotating stars, according to the recent simulations carried out by Julien et al. (1996). Our calculations show that the widening of the main-sequence may be due to rotational mixing, in stars having a typical velocity ($\sim 100 \text{ km s}^{-1}$).

4.2. Role of μ -gradients

In the preceding section, we described the global results obtained by solving the complete set of equations stated in §2, which include the effect of the composition gradients. Here we shall examine in more detail the particular role of these μ -gradients.

In Fig. 7, we show the diffusion coefficient at three different ages, for the two rotating models. For the “slow” model, the major contribution to diffusion is turbulent. Close to the convective core, we note a significant drop in the diffusion coefficient, which is due to the steep molecular weight gradient. The turbulent transport is affected, but it is not suppressed (cf. Eq. 11).

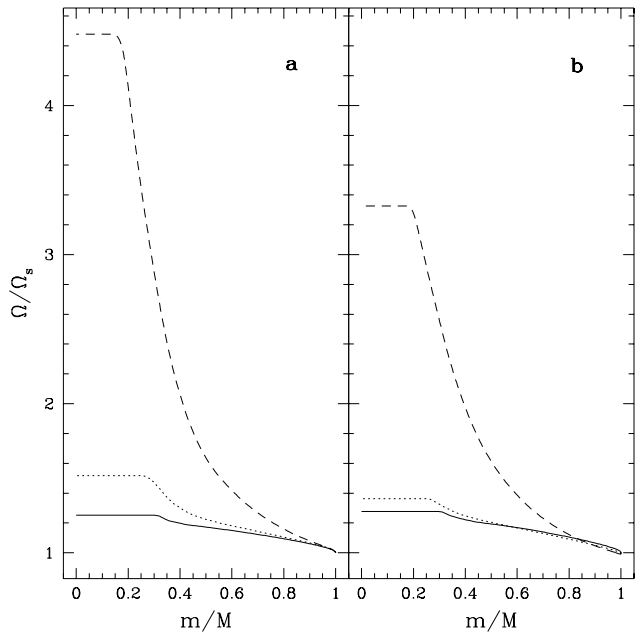


Fig. 8. Rotation profile and its variation with evolution. (Line styles are defined as in Fig. 7 and refer to the same models).

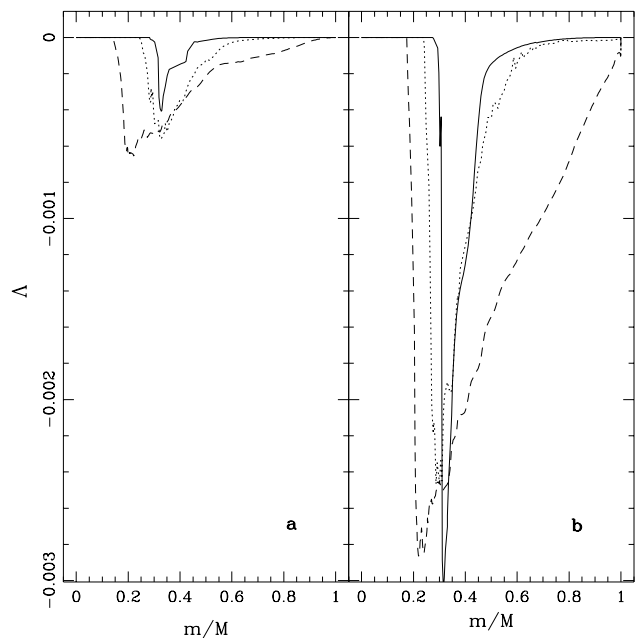


Fig. 9. $\Lambda = \tilde{\mu}/\mu$ and its variation with evolution. (Line styles are defined as in Fig. 7 and refer to the same models).

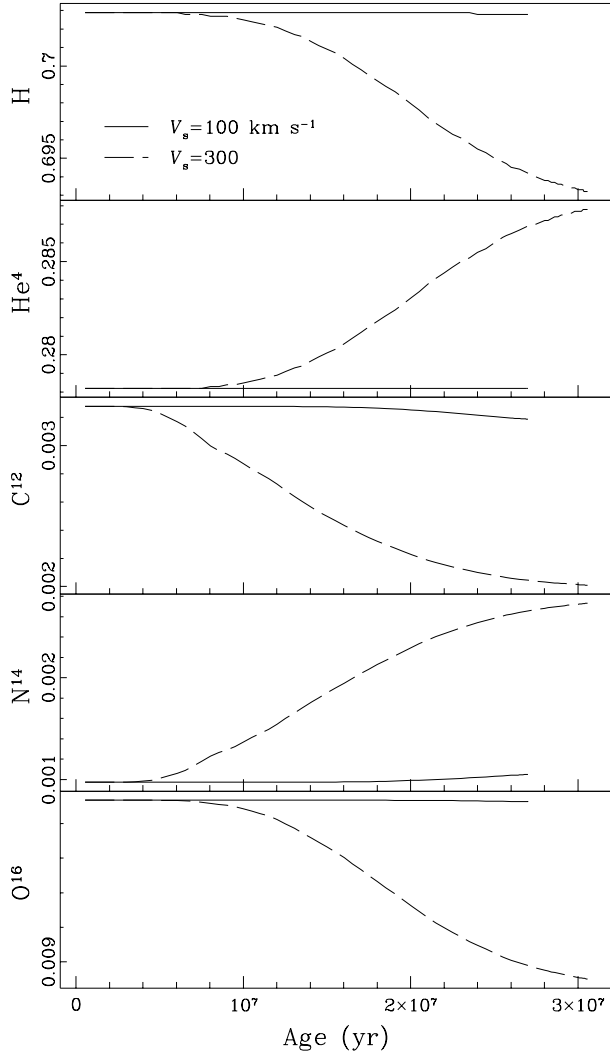


Fig. 10. Evolution of surface abundances. (Line styles are defined as in Fig. 5).

For the “fast” model, we note also a strong diminution of the diffusion coefficient near the surface. It is due to the reversed circulation cell, which grows with time. The reason for this growth is readily found; as the star evolves off the zero-age main-sequence, its radius grows and its breakup velocity decreases. Local conservation of angular momentum would lead to still faster decline of the surface velocity. However, circulation and turbulence keep extracting angular momentum from the interior, and the actual ratio between surface and critical velocities decreases.

The minimum of the total diffusion coefficient is thus located where $d\Omega/dr = 0$, and it reduces there to the effective diffusivity D_{eff} associated with the meridian cir-

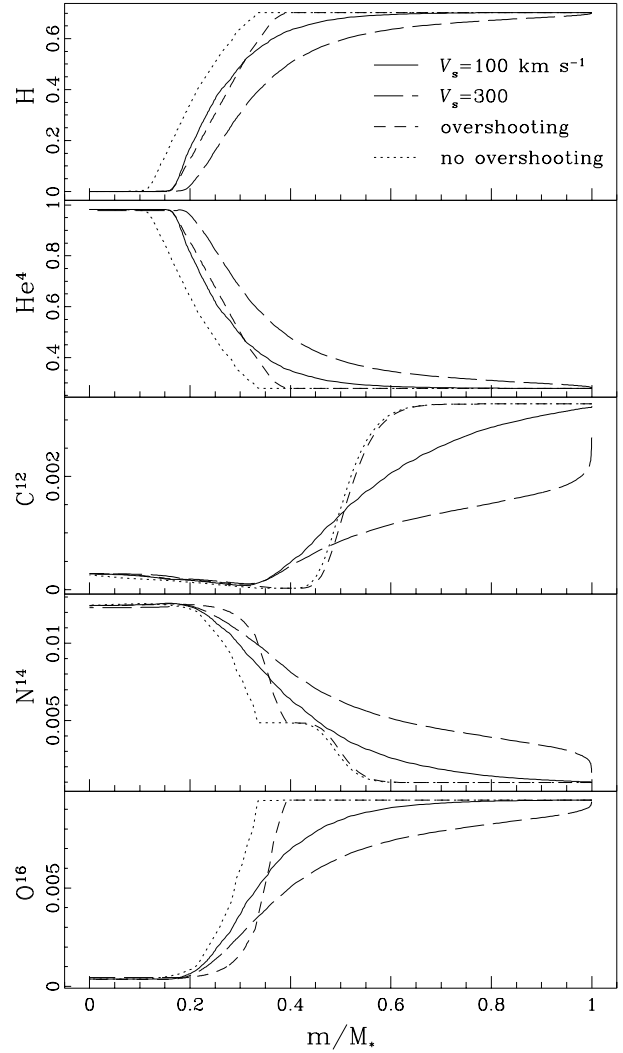


Fig. 11. Final abundance profiles on the TAMS of hydrogen (H), helium (He^4), carbon (C^{12}), nitrogen (N^{14}) and oxygen (O^{16}). (Line styles are defined as in Fig. 5).

ulation (cf. 9). That strangling will be the limiting factor in the modification of the surface abundances of the fast models (see also Figs. 10 and 11).

Another important effect is shown on the rotation profile within the model (cf. Fig. 8). It is clear that those profiles are quite different from what is required for thermal equilibrium (see Fig. 4). The main reason for this difference is the presence of the term in Λ (shown in Fig. 9). The steep profile in Λ requires that Θ be also very steep there, so that the sum of the two terms can give a profile similar to that shown in Fig. 4, which would be required for the asymptotic regime.

There is here an interesting coupling between all the variables. If $d\mu/dr$ is large, then so is Λ (cf. Eq. 8), and consequently, so is $d \ln \Omega/dr$. Such a strong differential rotation enhances turbulent diffusion, thereby diminishing $d\mu/dr$. However, as turbulent diffusion increases, so does U_r , and thus so does also Λ .

Let us stress that the behavior of Λ depends on an adjustable parameter C_h of order unity. That parameter is also present in D_v , through D_h (cf. Eq. 11). It is interesting to note that as C_h increases, so does Λ , but D_t varies in the opposite way. The net result is that the final profiles depend sensitively on the choice of C_h , which has here the value 0.15.

In Fig. 10, we show the evolution of the surface abundances of a few elements, and in Fig. 11, the final abundance profiles. Fast rotation is required to yield detectable abundance changes on the main-sequence. However, even for the “slow” model, the post-main-sequence evolution is probably affected by the composition changes inside the star. Furthermore, as mass loss becomes more important with the evolution off the main-sequence, additional changes of the surface abundances will occur through the “peeling” of the outer layers.

5. Discussion

We completed a first set of calculations of rotational mixing induced by meridional circulation as well as shear turbulence, with the rotation profile evolving consistently with these flows.

Unfortunately, very few observations permit to verify the full validity of the results. Gies & Lambert (1992) have observed galactic B stars and measured their rotational velocity, as well as their CNO abundances. However, they studied only slow rotators ($v \sin i < 85 \text{ km s}^{-1}$), which did not show strong evidence of composition changes.

One would expect binary systems to yield important information about the precise position in the HR diagram of stars with known masses, radii and rotation velocities. The best known binary in the $9 M_\odot$ mass range is QX Car, whose masses are $9.267 \pm 0.122 M_\odot$ and $8.480 \pm 0.122 M_\odot$ (cf. Andersen 1991). However, these stars are located too close to the ZAMS to give any interesting information about rotational mixing. Other binary systems (e.g. α Vir, NY Cep) are not known with sufficient precision to be used for any reliable comparison.

The most promising tests will be provided by the fastest rotating B-stars, which show signs of helium enrichment. The difficulty will be however to sort out the effects of semi-convection from those of rotational mixing.

Let us finally recall that a complete treatment of rotational mixing must include the angular momentum transport by the internal gravity waves emitted from the convective core. Such transport appears to be quite important in the Sun, as pointed out recently by Kumar & Quataert (1996) and by Zahn, Talon & Matias (1996). Since inter-

nal waves tend to restore uniform rotation, which would speed up the circulation, one expects a priori more mixing to occur. But the whole problem is highly non-linear, and it is difficult to make any prediction until this wave transport has been implemented and its impact has been evaluated. Work is progressing in this direction.

Acknowledgements. S.T. gratefully acknowledges support from NSERC of Canada.

References

- Andersen J., 1991, *A&AR* 3, 91
 Busse F.H., 1981, *Geophys. Astrophys. Fluid Dynamics* 17, 215
 Caughlan G.R., Fowler W.A., 1988, *Atomic Data Nuc. Data Tables* 40, 283
 Chaboyer B., Zahn J.-P., 1992, *A&A* 253, 173
 Clement M.J., 1979, *ApJ* 230, 230
 Denissenkov P., 1994, *A&A* 287, 113
 de Jager C., Nieuwenhuijzen H., van der Hucht K.A., 1988, *A&AS* 72, 259
 Eddington A.S., 1925, *Observatory* 48, 78
 Eryurt D., Kirbiyık H., Kızılođlu N., Civelek R., Weiss A., 1994, *A&A* 282, 485
 Gies D.R., Lambert D.L., 1992, *ApJ* 387, 673
 Gratton L., 1945, *Mem. Soc. Astron. Ital.* 17, 5
 Grevesse N., 1991, *A&A* 242, 488
 Henyey L., Forbes J.E., Gould N.L., 1964, *ApJ* 139, 306
 Herrero A., Kudritzki R.P., Vilchez J.M., Kunze D., Buttler K., Haser S., 1992, *A&A* 261, 209
 Iglesias C.A., Rogers F.J., Wilson B.G., 1992, *ApJ* 397, 717
 Julien K., Legg S., Mc Williams J., Werne J., 1996, *Dyn. Atmosph. Oceans* 24, 237
 Kippenhahn R., Thomas H.-C., 1970, in *Stellar Rotation*, IAU Coll. 4, Ed. A. Slettebak, 20
 Kumar P., Quataert, accepted by *ApJL*
 Kurucz R.L., 1991, in *Stellar Atmospheres: Beyond Classical Models*, NATO ASI Series C, Vol. 341, Eds. L. Crivellari, I. Hubeny, D.G. Hummer, p. 441
 Landré V., Prantzos N., Aguer P., Bogaert G., Lefevre A., Thibaud J.P., 1990, *A&A* 240, 85
 Langer N., 1991, *A&A* 243, 155
 Langer N., 1992, *A&A* 265, L17
 Maeder A., 1995, in *Astrophysical Applications of Stellar Pulsation*, IAU Coll. 155 (in press)
 Matias J., Talon S., Zahn J.-P., 1996 (preprint)
 Mestel L., 1953, *MNRAS* 113, 716
 Meynet G., Maeder A., 1996, *A&A* (in press)
 Öpik E.J., 1951, *MNRAS* 111, 278
 Roxburgh I., 1978, *A&A* 65, 281
 Roxburgh I., 1989, *A&A* 211, 361
 Schaller G., Schaerer D., Meynet G., Maeder A., 1992, *A&AS* 96, 269
 Stothers R.B., Chin C.W., 1991, *ApJ* 381, L67
 Talon S., Zahn J.-P., 1996, *A&A* (in press)
 Urpin V.A., Shalybkov D.A., Spruit H.C., 1996, *A&A* 306, 455
 Vogt H., 1925, *Astron. Nachr.* 223, 229
 Zahn J.-P., 1983, in *Astrophysical Processes in Upper Main Sequence*, 13th Saas-Fee Course, Eds. B. Hauck, A. Maeder.
 Zahn J.-P., 1991, *A&A* 252, 179
 Zahn J.-P., 1992, *A&A* 265, 115 (Paper I)

Zahn J.-P., Talon S., Matias J., 1996 accepted by A&A